Lasers in Manufacturing Conference 2025

Water and gas atomized AISI 316L powder for DED-LB: A comparative study on powder properties and build quality

Josefine Lemke[a,1], Max Biegler[a], Michael Rethmeier[b,a,c]

[a] *Fraunhofer Institute for Production Systems and Design Technology IPK, Pascalstrasse 8-9, 10587 Berlin, Germany*
[b] *Institut für Werkzeugmaschinen und Fabrikbetrieb IWF, Technische Universität Berlin, Strasse des 17. Juni 135, 10623 Berlin, Germany*
[c] *Bundesanstalt für Materialforschung und -prüfung (BAM), Unter den Eichen 87, 12205 Berlin, Germany*

Abstract

Powder properties are considered a key factor in part quality in laser additive manufacturing, although few studies have investigated the effects in directed energy deposition (DED). Water atomized (WA) and gas atomized (GA) powders are frequently used but may result in different part properties due to powder properties. To examine their qualification for DED-LB, this work examines powders and build quality of AISI 316L. Also, examination techniques are compared. The results show that the powder production has no relevant influence on porosity and Archimedian density of built parts. WA powders show good processability in DED-LB, despite unfavorable morphology. In contrast, WA specimen reach only 10% fracture elongation in tensile testing whereas GA-based specimen achieve 30%. Tensile strength of both is above 500 MPa. The reason for the lower mechanical property values can be attributed to defects and oxides. WA powders may provide a cost-effective alternative for DED-LB when mechanical load requirements are not important.

Keywords: DED-LB; porosity; AISI 316L; water atomized; gas atomized; powder

1. Introduction

Additive manufacturing (AM) has grown significantly in importance in recent years. Particularly noteworthy is the use of directed energy deposition (DED) in the maintenance, repair, and overhaul (MRO) of molds, dies, tools and turbine blades (Saboori et al., 2019). Recently there has been a significant expansion in the application of DED on the coating of brake discs due to novel environmental regulations, requiring the deployment of innovative technologies to ensure compliance with emission limits (Consilium, 2024). The AM industry is developing rapidly, with the use of AM for end-use parts already stated by 32% of companies in the 2024 Wohlers Report (ASTM International). The global growth of the AM market is evident when looking at market growth from 2022 to 2023: The market value of AM products and related services reached 20 billion in 2023, marking an 11% increase from 2022 (ASTM International). DED systems show enormous development potential, as only 6% of the revenue share of metal AM technology systems is covered by DED. The main market share is dominated by the laser-based powder bed fusion (PBF) technology with 82% (AMPOWER GmbH & Co. KG).

In particular, the powder-based DED-LB process shows immense potential. It can be used to apply material to large components, to recondition worn bearing seats or to additively manufacture 3D structures. Despite advances in technology, the correlation between the properties of powders and the quality of additively built components remains largely unexplored (Fedina et al., 2020). AISI 316L is one of the most frequently used materials in additive manufacturing, but the nature of the powder used is often not well understood. Factors such as the attachment of satellites, insufficient grain size in particle size distribution or differences in morphology of the particles can affect the melting behaviour and thus the resulting component quality. Hoeges et al. investigated water atomized (WA) powder in the PBF-process (Hoeges et al., 2017). The powders have a very unfavorable morphology but could be a cost-effective alternative to expensive GA powders.

* Corresponding author. Tel.: +49 30 39006 307.
E-mail address: josefine.lemke@ipk.fraunhofer.de

This leads to the question of whether high-quality results can be achieved with water-atomized (WA) powders, as with gas-atomized (GA) powders, for industrial applications with DED-LB.

2. State of the art

Several studies are dealing with laser-based powder bed fusion (PBF-LB). The VDI 3405 guideline even recommends a testing guideline for powders used in powder-bed processes (VDI, 2018). However, authors like Fedina et al. confirm that the influence of powder properties on component quality are rarely investigated (Fedina et al., 2020). This applies especially to DED-LB.

The most common method to atomize metal powder is using argon or nitrogen inert gas (Beiss, 2013). This process leads to particles that appear to be round with individual satellites. Processing gas-atomized particles can lead to the most common defects in the DED, i.e., gas pores as described in the review paper by Gushchina et al. (Gushchina et al., 2023). The authors point out a certain porosity to be normal for the DED process and not necessarily resulting in inadequate mechanical properties. Also, Snell et al. describe gas pores as the most common type of pores (Snell et al., 2020). They either originate from pores in the powder particles or from the process itself. In the case of lack of fusion, which can also be counted as porosity according to Snell et al., sharp edges and size have a higher impact on structural failure. However, this effect is less noticeable with spherical gas pores. For these reasons, the density of additively manufactured components according to Höges et al. is often used as a reference value to see whether desired mechanical properties can be achieved (Hoeges et al., 2017). In their work, Spierings et al. compare various measurement methods for determining the component density (Archimedes, micrograph analysis and X-ray scanning) (Spierings et al., 2011). They find very high accuracies for the Archimedian method. To compare measured density values, Vincic uses a reference density of 7.98 g/cm3 for AISI 316L (Vincic, 2023). He then builds components using DED and analyzes them using gas pycnometry to determine the component density with an average of 7.93 g/cm3.

Due to the atomization process, water atomization results in different morphological properties but is considerably more economical, as Riabov et al. motivate in their work (Riabov, 2022). The chaotic morphology happens due to the extremely high cooling rates of liquid metal meeting the water jet compared to the gas atomization process (Beiss, 2013). Yet, for DED-applications WA powders could offer a cost-effective alternative to gas atomization, especially for powder producing industries (Wielage et al., 2011). Also Pelz et al. investigate WA powders regarding their suitability for DED coating and thermal spraying (Pelz et al., 2012). They also emphasize the need for an economical alternative to expensive gas and plasma atomization processes. The cost advantage is derived by the process: WA can produce powders with up to ten times the melt flow rate of inert gas powders, which makes it economically interesting (Fedina et al., 2020). Another property to consider is the powders chemical composition. In particular, Hajnys et al. underline the presence of oxygen compounds to have a negative effect on the process and on the final part quality (Hajnys et al., 2020). Oxide formation can occur during the manufacturing process for both gas and especially water-atomized powders (Hoeges et al., 2017). Strondl et al. have written numerous works on powder characterization and its influence on AM. One of their studies deals with powders for PBF-LB. They also find a negative effect of oxygen content on the mechanical properties and, along with porosity, describe them as the biggest influencing factors (Strondl et al., 2015). In 2019, Deng et al. investigates oxygen inclusions in powder from austenitic steels that are processed using PBF-LB (Deng et al., 2020). In their work, they describe various types of oxides on as-received powders that were atomized using inert gas.

In their experimental work, Zheng et al. analyze the microstructure of DED-built specimen made of AISI 316L (Zheng et al., 2008). The columnar structure shows different characteristics at various positions in the sample: while the grain structure is finer near the substrate, it is coarser at higher levels, which is due to the different heat gradients according to the authors.

As the effects of powder atomization on DED-processing are not widely explored, the aim of this work is to conduct a comprehensive analysis of the GA and WA powders, including methods for measuring density, flowability and the presence of oxides, as well as the mechanical properties of DED-built samples. In addition, the microstructure is examined for the presence of defects. Particular attention is paid to qualifying morphologically unfavorable WA powders and evaluating their potential for use in additive manufacturing, especially with DED-LB.

3. State of the art

An experimental study was conducted in which water and gas atomized powders of austenitic stainless steel AISI 316L (EN 1.4404) were analyzed and applied in DED- LB build ups. The powders were obtained from different manufacturers and were processed without sieving or drying. The nominal grain sizes of the powder fractions were 20 µm - 63 µm for the GA powder and 38 µm - 63 µm for the WA powder, according to the specifications of the manufacturers. The powder fractions

were welded using DED-LB, and their relative component density was analyzed using Archimedes principle and digital image analysis on cross sections. Mechanical properties were investigated with tensile tests. Fixed parameter sets were used for the build-up of the specimen; parameter development and optimization were not the focus of the work.

3.1. Powder characterization: Morphology, particle size distribution, flowability and chemistry

Qualitative images were captured using a scanning electron microscope (Phenom XL G2 desktop SEM) including a secondary electron detector (SED) to visualize the topography. Dynamic image analysis (DIA) was used for the determination of the particle size distribution (PSD) and quantitative morphology with a CAMSIZER X2 from Microtrac MRB. To analyze the flowability of the powders, the flow rate of 50 g of powder in a calibrated funnel was determined using the Hall flow method in accordance with DIN EN ISO 4490. Each measurement was conducted three times, and results were averaged. Chemical analysis was obtained by inductively coupled optical emission spectrometry (ICP-OES) for GA powder, results for WA powder was provided from the manufacturer.

3.2. DED-LB build-up of specimen

To investigate the influence of the manufacturing method of the powders on component density, test specimen were built up from both powders, WA and GA. The experiments were carried out on a TruLaser Cell 7020 with 1.2 kW laser power, 500 mm/min weld speed and 3.8 g/min powder mass flow. The system is equipped with a Trumpf TruDisk laser (1030 nm) and a disc powder feeder. A three-jet nozzle was used. Figure 1 shows the schematic process for DED-LB welding.

3.3. Determination of part density and mechanical properties

The component density of the specimen was determined in accordance with the Archimedean principle as specified in DIN ISO 3369:2010. The measurements were conducted on a precision balance with an accuracy of $1x10^{-3}$ g. For each powder, three cubes were welded, and the component density was determined through three repeated measurements. Relative component density was also determined using digital image analysis based on one cross section of the test specimen. The image acquisition was performed on unetched specimen in a single plane and analyzed using algorithms. To accurately measure pore diameters, ImageJ was used to calibrate the image pixels according to their respective size. Mechanical properties were analyzed by performing tensile tests in accordance with DIN EN ISO 6892-1:2020-06 (EN ISO 6982-1:2019. Specimen geometry was configured with DIN 50125-E, measuring 2 x 3.1 x 15.

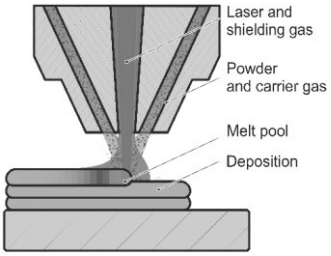

Figure 1: Deposition procedure (schematic) of DED-LB process.

4. Results and discussion

4.1. SEM-analysis of morphology and flowability

The qualitative visual analysis of the GA particles in Figure 2 (top) shows that most of the particles are round. Small particles in the 1 µm range are attached to them. Single large satellites appear occasionally, either attached to the particle surface or fused to the parent particle to form a common surface. Some agglomerates can also be seen, as well as a few deformed particles. Individual, very small particles < 10 µm are visible on the black background of the carbon pad. This indicates the presence of undersized particles. Undersize particles suggest an increased proportion of finer particles outside the nominal size distribution and can be disadvantageous for processability with DED-LB. Studies by Hoeges et al. emphasize that finer powders can flow less well due to the higher surface area and van der Waals forces (Hoeges et al., 2017). Since the particle size distribution for the powder is already quite small for DED-LB, this can result in a risk of poorer flow. The satellites and the many small particles can also have an influence on the processing parameters. Except for the undersized particles, the predominant particle size is still within the nominal range according to visual analysis.

As expected, the WA particles in Figure 2 (bottom) show a completely different external appearance. Their particles have no round shape but are irregular and without any recognizable pattern. On the other hand, no microparticles, very small particles or satellites can be seen here in contrast to the GA powder. The molten steel meets the water jet in the manufacturing process. The water causes the steel to solidify quickly due to its high cooling rate (Beiss, 2013). According to Pelz et al. a stable powder feeding especially in DED-LB and thermal spraying technologies is crucial and depends strongly on particle flowing behavior, which in turns depends strongly on morphology (Pelz et al., 2012). That is why WA powders

were suspected to be non-suitable for a stable DED-process, according to the authors. Therefore, a regular flow and processability is of particular interest for their application in the DED-process.

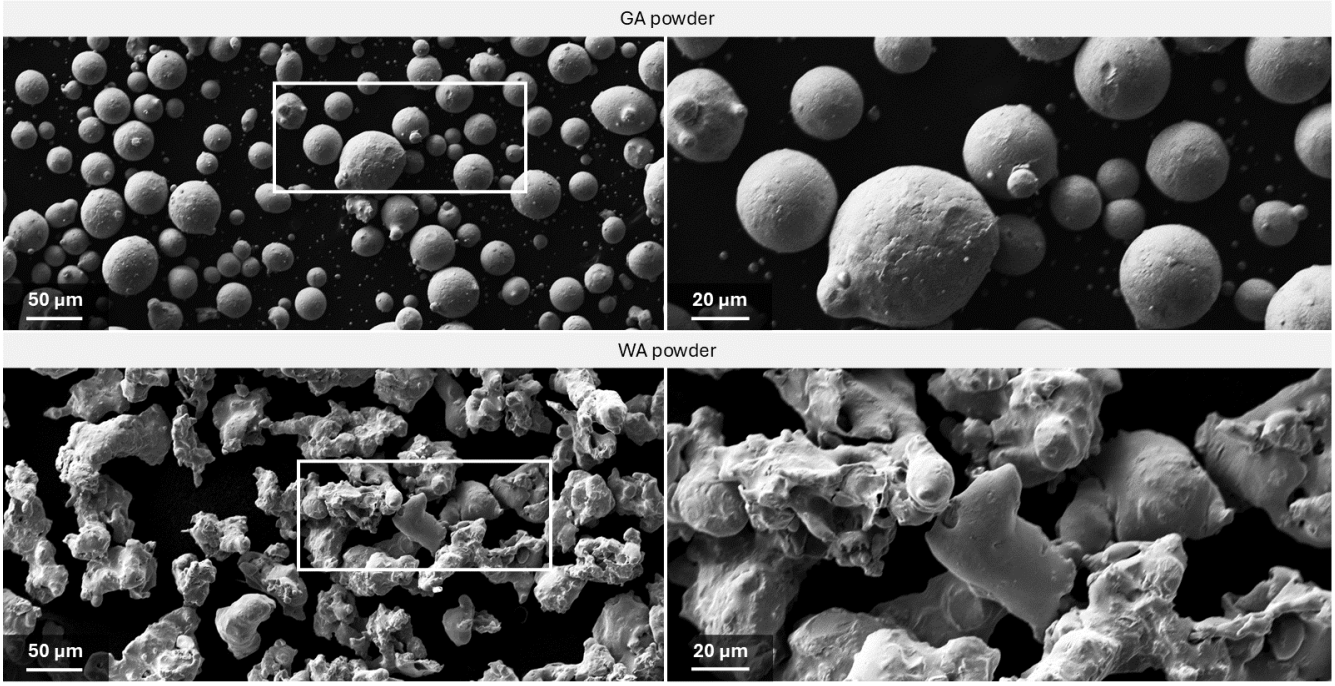

Figure 2: SEM-images with secondary electron detection of powders: GA (top) and WA (bottom).

The flowability analysis of the two powders using a Hall flow funnel is shown in Table 1. The WA powder flow is significantly slower than for the GA powder, as expected. The values correspond to those of Riabov, who also compares both powder production methods for AISI 316L (Riabov, 2022). He finds slightly lower values for WA powder with 37.4 s/50 g and GA powder flowing in the same range with 15.9 s/50 g. By contrast, the analysis by Hoeges et al. achieved significantly higher (and thus worse) values for GA with 21.5 s/50 g but again a quicker flowing of 34 s/50 g for a WA powder batch (Hoeges et al., 2017). For two other WA powders, Hoeges et al. do not achieve any flow using the Hall flow test, which indicates very poor flowability and underlines the limitations that WA powder processing can meet.

Table 1: Hall flow measurement results of water (WA) and gas atomized (GA) powders

AISI 316L Powder	Hall flow in 50 g/s
WA	42.0 ± 0.5
GA	15.5 ± 0,1

The reason for the differences between the two powder types from the GA and WA manufacturing processes originates in the very different morphology. For the WA powder, the interaction of the particles in motion when the funnel is opened results in an interlocking of the particles. They become entangled in each other in their chaotic structures. In addition, surface oxides, as is common with WA powders due to water atomization, can also can have an influence on flowability, as confirmed by Hoeges et al. (Hoeges et al., 2017). In contrast, the GA powder exits the funnel without difficulty and even exceeds the flow time observed in both comparative studies mentioned. The suspected poorer flowability cannot be concluded from the observed number of finer particles in the GA powder which was made in the SEM analysis.

4.2. Particle size and quantitative morphology approach

Figure 3 shows results for dynamic image analysis (DIA) of both powders. GA powder in black line and WA in grey. Left, the particle size and its relative distribution of both powders is compared. A visualization of the data as relative distribution is chosen to better visualize modes and span of the distributions. WA powder shows a distinct peak around 50 µm at the modal value, which represents the most common particle size in the examined sample. The distribution is symmetrical around the peak with only one mode. Most particles are found in the nominal range with no further outliers. In contrast, GA

powder distribution is coarser, with a more considerable proportion of smaller particles. The analysis shows two modes and a fair number of smaller particles below the expected threshold of 20 µm. This confirms the findings in the visual morphology analysis, compare Figure 2. Undersize phenomena are known to influence the flowing behaviour of the powders, which was not confirmed with regards to the Hall flow tests. A good performance of the GA powder is thus indicated despite the demonstrated number of smaller particles.

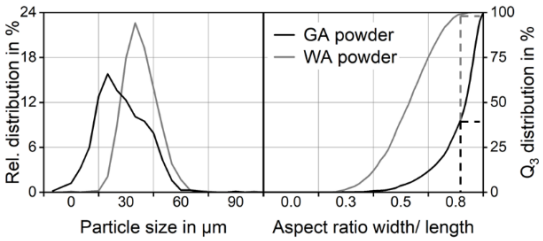

Figure 3: Particle size distribution as relative distribution and morphology factor aspect ratio for both powders GA and WA obtained by dynamic image analysis (DIA).

Hajnys et al. point out the necessary compromise between broad distributions for better packing density and narrow distributions that tend to flow better (Hajnys et al., 2020). For PBF applications, a bi-modality and broader distribution is recommended, as this leads to a more even distribution of the powder particles in the powder bed. However, this characteristic is rather less important for DED-LB, since the aim here is not to create a powder bed but to feed the powder in a uniform flow (Wielage et al., 2011). A bi-modal distribution as of the GA powder could thus possibly be disadvantageous for the DED-process. As the results of the flowability have shown, the GA powder flows well despite these considerations.

To evaluate morphology, in Figure 3 (right) the form factor aspect ratio provides quantitative evaluation of the particle shape. The aspect ratio describes the relation of width to length of a particle obtained by DIA. Via shadow projection, 2D-images of single particles can be obtained and automatically analyzed. A result of 1.0 would be achieved by a perfectly round shape (circle) (Microtrac Retsch GmbH, 2018). A chosen threshold of 0.9 is marked in Figure 3 (right) by a dashed line. The number of particles above this threshold are evaluated as round.

Results are as follows: In the examined GA powder sample, around 60% of particles are considered round (compare to black dash line: Number of particles between aspect ratio of 0.9 and 1.0). The majority of particles in SEM imaging (Figure 2) show satellites, which are altering the round basic shape. Also, elongated and deformed particles can be seen. This explains the comparably low number of 60% in relation to the round base shape of most particles.

In contrast to GA analysis, WA powder particles show values close to 0 for aspect ratio: Roundness can only be met by 1% of the particles. The results are as expected when looking at the morphology of the powders in Figure 2. These findings are as expected for WA powders as observed by other authors like Riabov (Riabov, 2022).

4.3. Welding results: microstructure and defects

Processing of WA powders was successful despite their morphology and flowability. There was no clogging of the nozzle during the build-up process, which is a promising result with regards to suspected processability issues of WA powders in DED (Wielage et al., 2011). The visual examination of the welded test specimen shows a good geometric reproduction of the cuboid shapes. Gushina et al. recommend a Hall flow rate for powders to be below 30 s for successful DED-process, which is successfully disproved by this study (Gushchina et al., 2023): Build-up was performed with WA powders of a flowability rate > 40 s, compare Table 1.

Figure 4 and Figure 5 show micrographs of DED-built specimen and detailed images. The cross-sections were etched with Beraha II for high-alloy chromium-nickel steels. The colour etching can be used to illustrate the different phases of AISI 316L. The grains are coloured according to their crystallographic orientation by the etching. As common in AM and especially in DED-LB, the individual weld beads can be identified. The schematic weld bead contour is dash lined in Figure 4 A. It shows the wave-like shape that is typical due to the set bead overlap. Each weld bead solidifies towards the outside from the centre, with the direction of heat dissipation running orthogonally to the circular shape of the individual beads. The direction of grain growth is opposite to the heat gradient (Zheng et al., 2008). The layers are repeatedly heated and the more layers there are, heat dissipation in downwards direction worsens. As a result, grains also grow across layers, which leads to the typical elongated grains and is what characterises the epitaxy of the structure. Less common in DED-LB as in cast structures are the equiaxed round grains. These are found sporadically in the lower area near the substrate, where heat dissipation is more rapid.

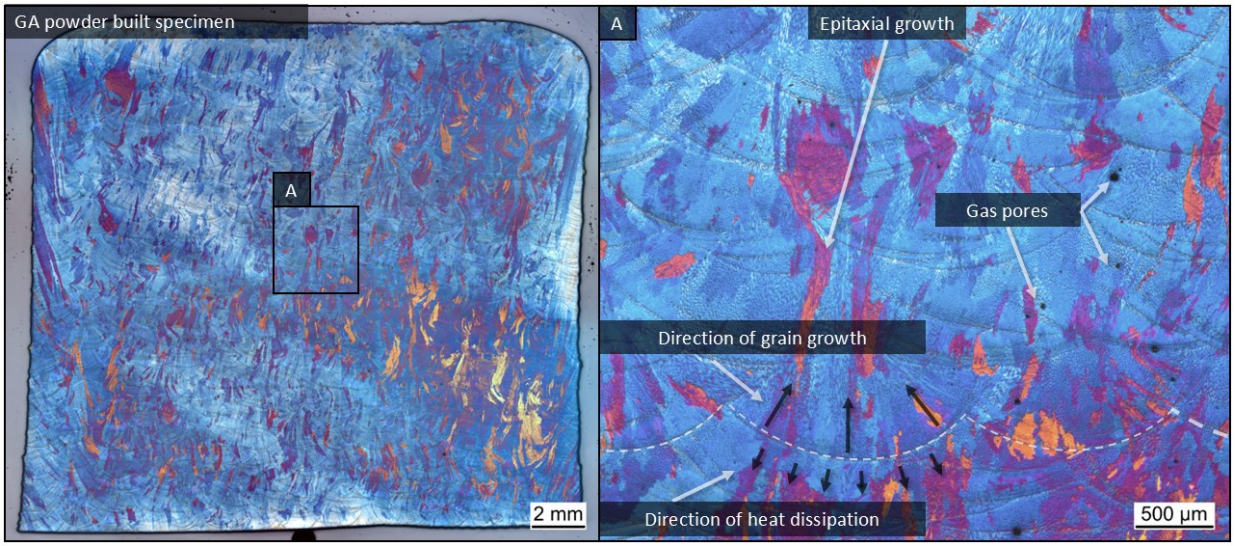

Figure 4: Cross section of DED-LB built specimen of GA powder, right: Detail views.

The GA specimen in Figure 4 contains finer and smaller grains than the WA specimen. These usually form when there is better heat dissipation or less heat in the overall component (Zheng et al., 2008). The WA specimen show defects, see Figure 5. Cracks occur between grains along the boundaries and through individual or multiple grains. One approach to explaining them can be found in the morphology of the powder. Due to the undefined structure with many folds and twists, the WA powder has a much larger surface compared to the GA powder. The GA powder particles with their basically round particles tend towards a more spherical shape that is preferred after atomization according to surface tension. Their spherical shape is more effective at reflecting the laser radiation, whereas the WA shape absorbs more energy. This way the WA powder might absorb more energy at the same power due to the higher surface to volume ratio. A higher energy absorption might lead to reduced cooling rates and thus enhanced grain growth, as described by other Zheng et al. (Zheng et al., 2008).

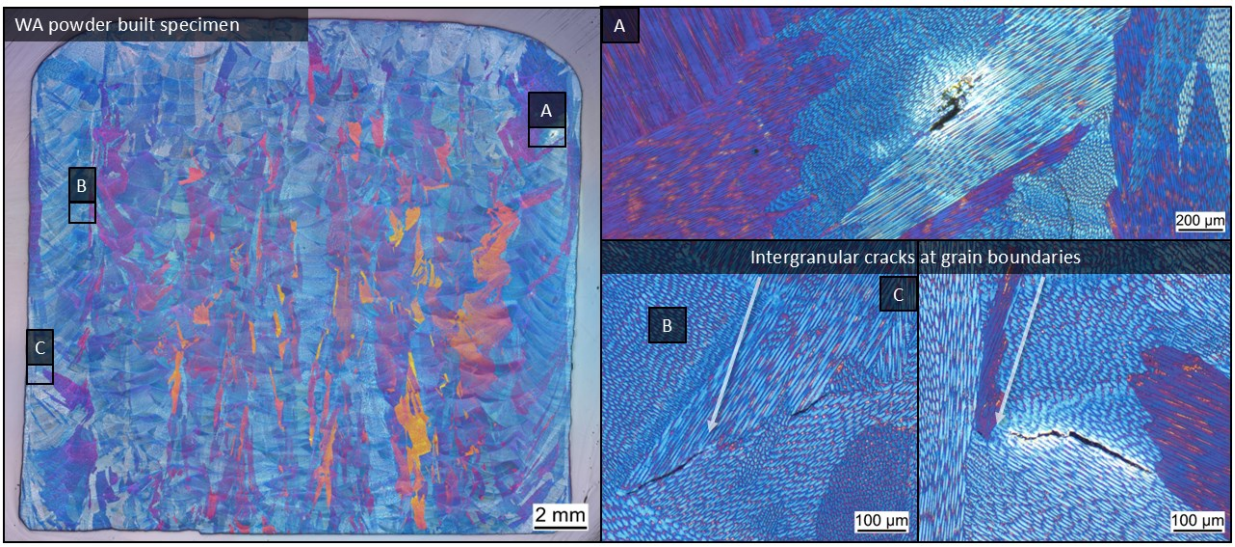

Figure 5: Cross section of DED-LB built specimen of WA powder, right: Detail views.

In their comparative study of WA and GA powder in PBF-LB, Fedina et al. also find a correlation between powder morphology and melt pool shaping due to the interaction with the laser beam (Fedina et al., 2020). The authors mention the particles surface to influence the laser interaction in the powder bed. In their investigations of the absorption of laser radiation, Hatem et al. also find differences in the melting behaviour of WA and GA powders (Hatem et al., 2021). They see

higher absorption for WA powder and suspect a correlation between the morphology and laser absorption. In the present examinations, despite defects due to suspected higher energy absorption, no pores can be found in the WA structure whereas single pores can be found in the GA, as are common for DED-LB (Gushchina et al., 2023). On the other hand, no defects can be seen in the micrographs of the GA specimen.

4.4. Chemical composition and oxides

The results for chemical analysis of the powders are shown in Table 2. The table shows also comparison to the standardized chemical composition in DIN EN 10088-3 for austenitic stainless steel AISI 316L (EN 1.4404).

Table 2: Chemical composition of GA (gas atomized) and WA (water atomized) powders obtained by ICP-OES. Information for WA provided from the manufacturer. DIN EN 10088-3 for comparison.

	Mo	Ni	Mn	Si	Cr	Fe	C
AISI 316L GA	2.2	10.2	1.14	0.7	15.6	Bal.	-
AISI 316L WA	2.2	12.4	0.3	0.5	17.8	Bal.	0
DIN EN 10088	2.0 2.5	10 13	0 2.0	0 1.0	16.5 18.5	Bal.	Max. 0.03

For GA powder, the amount of chromium is slightly decreased with 15.6% with regards to lower limits of standard DIN EN 10088. Also, increased manganese amounts can be found, which are still in the allowed range. In the production of AISI 316L powders, manganese and silicon can be used as oxide binders, which react with the oxygen according to Deng et al. (Deng et al., 2020). In their work, the authors were able to determine that the production of powders without manganese and silicon led to an increased oxygen concentration in the powder particles. This confirms the function of the binder elements. However, it is possible that these bound oxides become part of the powder particles.

For further investigation, individual particles of the powder samples were analyzed by SEM using back scattered electron detection (BSE), results see Figure 6. The particle of the GA powder shows dark spots, which are suspected to be oxides. According to Deng et al., density differences detected by BSE can qualitatively verify oxides in the metal matrix of the AISI 316L particle surfaces (Deng et al., 2020). Here, an obvious lack of iron and increased presence of oxygen, manganese, and silicon (compare DIN EN 10088-3 in Table 2) is visible. Manganese and silicon should only be present at 2 wt% and 1 wt%.

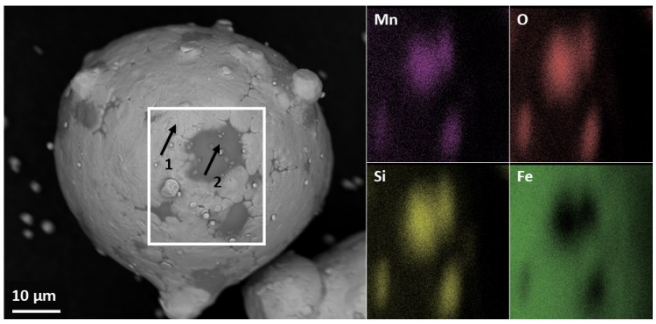

Figure 6: Detailed view on particle of GA powder in EDX BSE analysis with density differences (darker regions) and line scan positions.

Line scan results are shown in Table 3. In line scan 2 across the dark region, the presence of manganese and silicon is greatly increased at 22 wt% and 16 wt%. Also, the oxygen concentration is much higher and a difference in composition can be derived from the dark appearance in the BSE detection. In the work by Vincic, individual AISI 316L particles are also analyzed using SEM (Vincic, 2023). In this case, dark spots are also visible and clearly analyzed as oxides. Using SEM, the author determines 22% oxygen as in the present examination. The authors find oxides on the powder particles to be responsible for significant reduction of mechanical properties in their study. A reduced iron concentration with increased manganese and silicon indicates the presence of manganese and silicon oxides. According to Hoeges et al. oxygen in AISI 316L powders can lead to SiO_2, MnO and Cr_2O_3 (Hoeges et al., 2017). The presence of speckled oxide on surface is not unusual in the case of GA powder. However, it is a quality disadvantage that can lead to poorer mechanical properties. Gushina et al. criticize that the oxygen content is often not regulated by guidelines (Gushchina et al., 2023). In their review paper the authors also mention an increased amount of oxygen to indicate the presence of oxide inclusions on the surface and inside

the powder. The analysis with SEM is therefore useful for a first insight, even if it does not provide a quantified statement about the occurrence of oxygen. An elaborated gas analysis for final oxygen determination shall be accompanied by it.

Table 3: Linescan results of GA particle positions on surface (1) and on darker region (2)

Element	O	Si	Cr	Mn	Fe	Ni	Mo
wt% line scan 1	2.2	0.5	14.4	2	65.4	13.1	2.4
wt% line scan 2	22.7	15.6	18.5	21.7	19.6	1.3	0.6

4.5. Part density

To examine the density of the solid matter of the constructed samples, the components were analyzed using the Archimedes principle. The relative density allows a direct comparison with a selected target material. However, the reference values have a high impact on determination of the relative density. Figure 7 shows the results of relative and absolute Archimedean measurements compared with the density according to the pore analysis on the micrograph. Assuming a value of 8.0 g/cm^3 according to DIN EN 10088-1, the test specimen achieve relative densities of 99.8% for GA (DIN, 2024). A comparison with the results from the porosity analysis on the micrograph shows that the two measurements are in particularly good agreement. The high result of the micrograph analysis is consistent with the analysis of the micrographs, which show a small number of pores and no other defects, see section 4.3 on microstructure and defects. The deviation between relative density of Archimedes to relative density of the micrograph is < 1%. This corresponds well to the range found by Spierings et al. for deviations between micrograph analysis and Archimedes at high density values (Spierings et al., 2011).

Differences are more visible in the WA powder, where 99% relative density is achieved and thus lower values than for GA powder. Whereas the difference between micrograph and Archimedes is significantly larger, which results from the detection method. In image analysis, the porosity was detected using a connected components algorithm. The cracks are quite different in their characteristics, orientation and size and were not analyzed using image analysis. Therefore, the voids connected to the cracks are not detected by the image analysis. These then become even more visible using the Archimedean method, which therefore clearly demonstrates its usefulness.

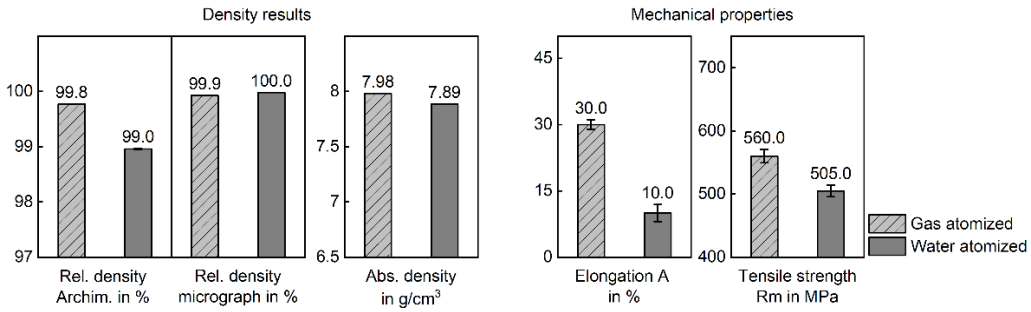

Figure 7: Left: Results for part density analysis; right: Results of tensile tests of WA and GA powder-built specimen.

In the work by Hoeges, densities of 99.84% are achieved using the Archimedes method for GA and 99.77% for WA powders (Hoeges et al., 2017). However, a specification of the reference value is not given. The values determined by the authors for the GA powders are in the same range as those from this study; the WA powders achieve slightly higher densities.

When considering the absolute density, the differences between the two powders show again: GA achieves 7.98 g/cm^3 and WA 7.89 g/cm^3. The values for the GA specimen exceed the average densities of the DED-built test specimen measured by Vincic (Vincic, 2023). In his work, he assumes a reference density of 7.98 g/cm^3. Regarding the comparability of the relative densities, a wrong conclusion would be made here using this reference. The author also presents absolute densities with 7.93 g/cm^3 on average, which can be slightly exceeded by this work comparing the GA powder-built specimen. At these remarkably high densities around 99%, differences lie in the decimal range and results would be misleading with using the references by Vincic. Other works do not specify any reference, making it difficult to classify and compare the relative densities achieved, what makes the absolute density assessment necessary.

4.6. Mechanical properties

The specimen made of WA and GA powder were analyzed with tensile tests. The results for ultimate tensile strength (UTS) and elongation at break A can be seen in Figure 7, right. In DIN EN 10088-3 the values for UTS and elongation are 500 MPa to 700 MPa and 40% elongation at break for AISI 316L (DIN, 2014). Regarding the additively manufactured specimen of this work, lower limits for UTS are met by both powders but elongation does not reach the desired values. In their comparative study of WA and GA powders, Höges et al. manufacture samples with PBF-LB. They achieve higher values for both powder samples: Elongations of up to 35% and tensile strengths of up to 620 MPa (Hoeges et al., 2017). Contrary to the authors suggestion by taking porosity as a value for evaluating if mechanical properties can be met, a deviation can be seen in this case. In contrast to the very good porosity values for both powders, mechanical properties are low. Reasons for this can be found in different explanations for the two powders examined.

The GA powder showed more oxides than usual in the SEM examinations. According to Hajnys et al., oxides can lead to lower strength and fatigue (Hajnys et al., 2020). The presence of atypical oxides in the GA powder can hence be taken as an explanation for why the UTS of the as-built specimen are lower than in comparison with the state of the art. Also Vincic discovers oxides on GA powder particles and assumes oxides on the particle surface to be the cause of a lower elongation (Vincic, 2023). Strondl et al. have published numerous works on powder characterization and its influence on additive manufacturing techniques. They also find the effect of oxygen content on the mechanical properties and describe them as the biggest influencing factors, along with porosity (Strondl et al., 2015). Since porosity is at high levels in the current work, oxides need to be considered as a reason for lower mechanical properties. Although no influence of the spherical gas pores can be derived on the mechanical properties of the WA specimen, the sharp edges factor of lack of fusions can be a mechanism that also happens describes cracks sharp edges (Snell et al., 2020). According to the authors, sharp edges can lead to a high impact on structural failure. Regarding the very low elongation at break in WA powder specimen, the defects and cracks found in the microstructure can be considered as responsible phenomenon. As discussed in the microstructure analysis, melt pool stability influences solidification and thus the microstructure (Hatem et al., 2021).

5. Conclusion

In the present study, water (WA) and gas atomized (GA) powders of AISI 316L were examined and successfully built up with DED-LB. Both powders can be processed well and were used to produce DED-printed specimen. Cheaper WA powders as stated as a need for DED-LB like Pelz et al. emphasize can thus be applied and be an alternative to cost intense GA powders (Pelz et al., 2012). The following results have been achieved:

- The size distribution of the GA powder particles shows an increased number of fine particles. This does not lead to a reduction of the flow properties. On the contrary, the measured Hall flow is good for fine GA powders with 15 s/ 50 g.
- The GA powder achieved UTS of 560 MPa within the target values of DIN EN 10088 for AISI 316L. Yet, elongation is lower than expected with 30%. An unusual finding of oxides on the GA powder particles surfaces can be a reason for the lower mechanical properties.
- Despite the very slow Hall flow of > 40 s/ 50 g and chaotic morphology of particles, the WA powder could be processed well. It resulted in a stable build-up.
- The mechanical properties of WA built specimen were lower than those of the GA. UTS is with 500 MPa still within the standard, but elongation is significantly too low. Low elongation is mainly attributed to defects that appeared in the microstructure.

Acknowledgements

The research project 01IF22325N “Effiziente Pulverqualifizierung beim additiven Aufbau mittels LPA” from DVS e.V., Düsseldorf, is funded via the DLR Projektträger within the framework of the program for Industrial Collective Research ("Industrielle Gemeinschaftsforschung", IGF) by the Federal Ministry of Economic Affairs and Climate Action based on a resolution of the German Bundestag. The project is carried out at Fraunhofer Institute for Production Systems and Design Technology.

References

Saboori, A., Aversa, A., Marchese, G., Biamino, S., Lombardi, M., Fino, P., 2019. Application of Directed Energy Deposition-Based Additive Manufacturing in Repair. Applied Sciences 9 (16), 3316.

Consilium, 2024. Euro7: Rat nimmt neue Vorschriften über Emissionsgrenzwerte für Pkw, leichte Nutzfahrzeuge und Lastkraftwagen an.
ASTM International. Wohlers Report 2024: 3D Printing and Additive Manufacturing Global State of the Industry, 195 pp.
AMPOWER GmbH & Co. KG. AMPOWER Report 2023, 153 pp.
Fedina, T., Sundqvist, J., Powell, J., Kaplan, A.F., 2020. A comparative study of water and gas atomized low alloy steel powders for additive manufacturing. Additive Manufacturing 36, 101675.
Hoeges, S., Zwiren, A., Schade, C., 2017. Additive manufacturing using water atomized steel powders. Metal Powder Report 72 (2), 111–117.
VDI, 2018. VDI 3405 Blatt 2.3, Strahlschmelzen metallischer Bauteile Charakterisierung von Pulverwerkstoffen: Additive Fertigungsverfahren. VDI-Gesellschaft Produktion und Logistik (GPL) 25.030, 17 pp.
Beiss, P., 2013. Pulvermetallurgische Fertigungstechnik. Springer Vieweg, Berlin, Heidelberg, 316 pp.
Gushchina, M., Klimova-Korsmik, O., Turichin, G., 2023. Features of the Powder Application in Direct Laser Deposition Technology, in: , New Advances in Powder Technology [Working Title]. IntechOpen.
Snell, R., Tammas-Williams, S., Chechik, L., Lyle, A., Hernández-Nava, E., Boig, C., Panoutsos, G., Todd, I., 2020. Methods for Rapid Pore Classification in Metal Additive Manufacturing. JOM 72 (1), 101–109.
Spierings, A.B., Schneider, M., Eggenberger, R., 2011. Comparison of density measurement techniques for additive manufactured metallic parts. Rapid Prototyping Journal 17 (5), 380–386.
Vincic, J., 2023. Laser Directed Energy Deposition for Processing and Repairing Steels. Dissertation, Torino, 173 pp.
Riabov, D., 2022. Laser-based powder bed fusion of stainless steel: Powder properties, processability and microstructure, 78 pp.
Wielage, B., Rupprecht, C., Gebert, G., Wocilka, D., Lindner, T., Kunze, M., Franik, D., 2011. Wasserverdüste Pulver für Auftragschweiß- und thermische Spritzprozesse. Schweißen und Schneiden 2011 (Ausgabe 7), 380–383.
Pelz, A., Bröer, F., Reichmann, B., 2012. Einsatz von wasserverdüsten Pulvern zum Auftragschweißen und Thermischen Spritzen. Vortrag bei der Schweißtechnischen Lehr- und Versuchsanstalt (SLV), Thale 2012.
Hajnys, J., Pagac, M., Mesicek, J., Petru, J., Spalek, F., 2020. Research of 316L Metallic Powder for Use in SLM 3D Printing. Advances in Materials Science 20 (1), 5–15.
Strondl, A., Lyckfeldt, O., Brodin, H., Ackelid, U., 2015. Characterization and Control of Powder Properties for Additive Manufacturing. JOM 67 (3), 549–554.
Deng, P., Karadge, M., Rebak, R.B., Gupta, V.K., Prorok, B.C., Lou, X., 2020. The origin and formation of oxygen inclusions in austenitic stainless steels manufactured by laser powder bed fusion. Additive Manufacturing 35.
Zheng, B., Zhou, Y., Smugeresky, J.E., Schoenung, J.M., Lavernia, E.J., 2008. Thermal Behavior and Microstructure Evolution during Laser Deposition with Laser-Engineered Net Shaping: Part II. Experimental Investigation and Discussion. Metall and Mat Trans A 39 (9), 2237–2245.
Microtrac Retsch GmbH, 2018. Bedienungsanleitung Auswertesoftware CAMSIZER® X2, 210 pp.
Hatem, A., Schulz, C., Schlaefer, T., Boobhun, J.T., Stanford, N., Hall, C., 2021. Influence of laser absorption by water- and gas-atomised powder feedstock on Laser Metal Deposition of AISI 431 stainless steel. Additive Manufacturing 47, 102242.
DIN, 2024. DIN EN 10088-1: Nichtrostende Stähle - Teil 1: Verzeichnis der nichtrostenden Stähle; Deutsche Fassung EN 10088-1:2023, 80 pp.
DIN, 2014. DIN EN 10088-3: Nichtrostende Stähle - Teil 3: Technische Lieferbedingungen für Halbzeug, Stäbe, Walzdraht, gezogenen Draht, Profile und Blankstahlerzeugnisse aus korrosionsbeständigen Stählen für allgemeine Verwendung; Deutsche Fassung EN 10088-3:2014. Accessed 21 February 2023, 60 pp.